Journal of
Computational and Theoretical Nanoscience
Vol. 3, 1–7, 2006

Molecular Conduction Characteristics from the Intrinsic Molecular Properties

Nikita Matsunaga

Department of Chemistry and Biochemistry, Long Island University, Brooklyn, NY 11201, USA

Virtual orbitals with valence character are constructed from quasiatomic minimal basis set molecular orbitals. The virtual orbital energies determined in this way are basis set independent. Such orbital energies are used here to understand the low-energy conduction of molecules for which experimental studies are available. The experimental conduction energy correlates well with the lowest unoccupied molecular orbital for molecules ranging from a hydrocarbon to phenylene ethynylene oligomers.

Keywords: Molecular Electronics, HOMO-LUMO Gap, Quasiatomic Minimal Basis Orbitals, Valence Virtual Molecular Orbitals.

1. INTRODUCTION

By far the most popular and important theoretical techniques for investigations in molecular electronics are those based on non-equilibrium Green's function methods[1] (NEGF). The NEGF method solves for the non-equilibrium spectral density, and the density is subsequently used to obtain transmission probability that appears in the Landauer expression of current, I, as a function of applied voltage, V,

$$I = \frac{2e}{h}\int_{-\infty}^{+\infty} T(E,V)[f(E-\mu_i(V)) - f(E-\mu_f(V))]\,dE \quad (1)$$

Here $T(E,V)$ is the energy- and voltage-dependent transmission probability and f is the Fermi function. The $\mu(V)$ factors in the arguments of the Fermi function are the chemical potentials of each electrode, labeled with subscripts i and f. The Landauer current expression solved by the NEGF method has now been applied at various levels of theory that range from the tight binding Hückel Hamiltonian[2] to Hartree-Fock[3] and density functional theory.[4]

While the development of the NEGF-based method is very useful as it has enormous potential for predictive power in the field of molecular electronics, it would be also helpful to seek a simpler approach that is motivated in a more intuitive way using intrinsic physical or chemical properties. Only a handful of articles that have appeared in the past report techniques motivated by physical/chemical properties.[7–9]

The system we would like to examine ultimately is shown in Figure 1. Here a molecule is sandwiched between two electrodes that are connected to an electrical circuit. The electrodes are semi-infinite in size and, therefore, they possess band structures. The molecule in the junction, (with discrete energy levels) is connected to the electrodes by either covalent bonds, weaker interactions such as van der Waals, or both. When a voltage is applied across the two electrodes, the electrons with energies in resonance with the molecular orbitals (MOs) are transported across the electrodes. From this rather crude view, one can see that the conduction characteristics of a molecular electronic device are dominated by two factors: (1) the connectivity of the molecule in the junction, and (2) molecular energy levels. The former is system dependent and is very difficult to assess unless calculations are performed to solve Eq. (1) in numerous different nuclear configurations of differing sizes and shapes.[10] On the other hand, understanding the molecular energy levels, which the electrons are piped into, is easier to deal with. Questions such as those given below can be answered by standard electronic structure calculations:

(1) Is it possible to predict *a priori* the lowest potential at which conduction begins to occur?
(2) How many channels are there in a given energy region?
(3) How does chemical substitution change conduction characteristics?

In the present article, we attempt to answer these questions by examining the intrinsic properties of the molecules with first-principle electronic structure calculations.

The so-called frontier orbital energies are quite important in chemical reactivity.[11, 12] The frontier orbitals consist of the highest occupied MOs (HOMO) and the lowest unoccupied MOs (LUMO). A chemical reaction proceeds by interaction of the HOMO of one reactant and the

RESEARCH ARTICLE

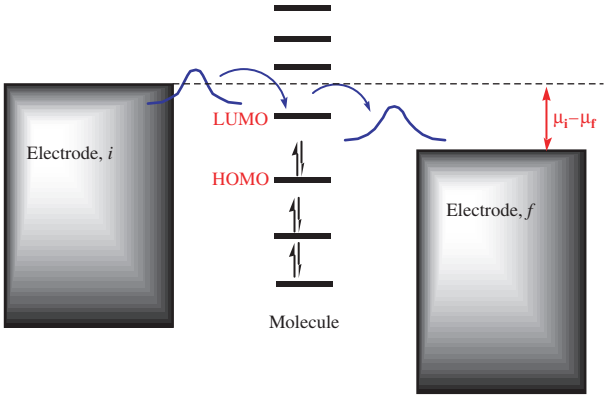

Fig. 1. A model system of a molecular electronic device. The molecule is either covalently or weakly bound to the two electrodes. When a voltage, V^{app}, is applied across the electrodes such that $V^{app} = \mu_i - \mu_f$, the LUMO of the molecule becomes in resonance with the electrons in the electrode i, resulting transfer of electrons.

LUMO of the other. For example, a class of reactions called Diels-Alder reactions is entirely understood in its mechanistic and energetic aspects by examining the interaction between the frontier orbitals of the reactant molecules.[13] In the case of nanoelectronics, the low energy conduction should also be concerned with the frontier orbitals. In addition, from the crude view of Figure 1, it is clear that the applied voltage, an energetic width that is the difference $\mu_i - \mu_f$, can encompass several low-lying orbitals. Therefore, it is interesting to see how the electronic structure theory can help understand the low-lying unoccupied orbitals.

The role of frontier and low-lying unoccupied or virtual orbitals in the Hartree-Fock (HF) theory and the density functional theory (DFT) is not obvious. In fact, the virtual orbitals have no physical meaning since they are not optimized in the calculations. Furthermore, the virtual orbital energies are basis set dependent.[14b] The virtual orbital energies can change drastically with the addition of more basis functions to achieve convergence of relative energy in the molecular system. Thus, the virtual orbitals may not be suitable for analyzing the energetic location of the unoccupied orbitals.

In the present article, we construct the virtual orbitals of the HF theory and DFT in a basis set independent way. In the following section, the quasi-atomic minimal basis orbital method to obtain valence virtual orbitals is explained. This technique is then employed to address the issue of basis set dependence of the virtual orbitals.

2. THEORETICAL METHOD

The method described below gives basis set independent unoccupied orbitals with valence character. The method was derived by Ruedenberg and co-workers.[14] Here the description of the method is given briefly only to catch the essence of the method. More complete discussion and details of implementation are found in Ref. [14].

2.1. Quasiatomic Minimal Basis Set Orbitals (QUAMBO)

The essence of the method is to obtain molecular orbitals that deviate as little as possible from the free-atom minimal basis valence reference atomic orbitals. The free atom minimal basis atomic orbitals are projected onto the space spanned by the canonical Hartree-Fock (or DFT) molecular orbitals (MOs). These projected minimal basis atomic orbitals are then used to evaluate the transformation of the MOs to the QUAMBO by minimizing the mean square deviations of the transformed MOs and the projected free atom minimal basis valence AOs.

We start by defining the free atom minimal basis AO, A_j^* in terms of occupied, labeled by the subscript n, and virtual, labeled by the subscript v, MOs obtained by the Hartree-Fock or DFT method,

$$A_j^* = \sum_n \varphi_n a_{nj}^* + \sum_v \varphi_v a_{vj}^* \tag{2}$$

where φ are the Hartree-Fock MO's and a^* represents the projection operator, expressed as $a_{nj}^* = \langle \varphi_n | A_j^* \rangle$ and $a_{vj}^* = \langle \varphi_v | A_j^* \rangle$, that projects the free atom AO's onto the MO's. The label for the occupied orbitals, n, runs from 1 to N, and v from $N+1$ to V.

The QUAMBO of a molecule can also be expanded in terms of occupied and virtual MOs,

$$A_j = \sum_n \varphi_n a_{nj} + \sum_v \varphi_v a_{vj} \tag{3}$$

where $a_{nj} = \langle \varphi_n | A_j \rangle$ and $a_{vj} = \langle \varphi_v | A_j \rangle$. Here v is the number of virtual orbitals in a minimal basis; it spans the whole virtual orbital space. Since the quasiatomic virtual orbitals have the minimal basis nature, only the subset of the whole is needed. The QUAMBO, A_j should then be rewritten as

$$A_j = \sum_n \varphi_n a_{nj} + \sum_p \psi_p a_{pj} \tag{4}$$

where p runs from $N+1$ to $P =$ number of virtual orbitals in the minimal basis, with $P < V$. The ψ_p is expressed as

$$\psi_p = \sum_v \varphi_v T_{vp} \tag{5}$$

Here T_{vp} is a rectangular matrix transforming the canonical MOs, φ_v, to ψ_p with the property

$$\sum_v T_{vp} T_{vq} = \delta_{pq} \tag{6}$$

Thus, once T_{vp} is obtained QUAMBO can be constructed.

The transformation matrix is obtained by minimizing the mean square deviation of the transformed MOs and the projected free atom minimal basis valence AOs with the constraint that MOs are normalized, $\langle A_j | A_j \rangle = 1$. The constraint minimization is accomplished by the Lagrange multiplier method, and the mean square deviation can then be derived as,

$$\langle A_j - A_j^* | A_j - A_j^* \rangle = 2(1 - D_j^{1/2}) \tag{7}$$

RESEARCH ARTICLE

where

$$D_j = \sum_n \langle \varphi_n | A_j^* \rangle^2 + \sum_p \langle \psi_p | A_j^* \rangle^2 \quad (8)$$

Ultimately, maximizing the sum over p space alone suffices for constructing virtual valence orbitals, (VVOs). The sum, s, is given as

$$s = \sum_j \sum_p \langle \psi_p | A_j^* \rangle^2 = \sum_p \sum_v \sum_w T_{vp} T_{wp} B_{vw} \quad (9)$$

where B_{vw} is given by

$$B_{vw} = \sum_j \langle \varphi_v | A_j^* \rangle \langle \varphi_w | A_j^* \rangle = \sum_j a_{vj}^* a_{wj}^* \quad (10)$$

with

$$j = 1, 2, \ldots, M = N + P$$

$$p = 1, 2, \ldots, P$$

$$v, w = N+1, N+2, \ldots, N+V$$

The transformation matrix **T** is determined from an eigenvalue equation,

$$\sum_w B_{vw} T_{wp} = \beta_p T_{vp} \quad (11)$$

with the largest $N + P$ eigenvalues β_p maximizes the s.

The VVOs energies are obtained by diagonalizing the Fock matrix of the form,

$$\langle \psi_p | \mathbf{F} | \psi_q \rangle = \sum_v \varepsilon_v T_{vp} T_{vq} \quad (12)$$

where ε_v is the virtual orbital energy of the canonical HF orbitals.

2.2. Computational Details

Nitrobenzene is chosen to examine both the relationship between canonical orbitals and the VVOs derived from the QUAMBO and the convergence of the virtual orbitals. The geometry of the nitrobenzene examined is fully optimized at the RHF level of theory with the respective basis set (*vide infra*), represented by the notation RHF/basis. The RHF optimized geometry is used for the DFT calculations with the corresponding basis set. The functional chosen for DFT calculations is so-called B3LYP functional[15] which utilizes the three-parameter exchange functional of Becke[16] and the correlation functional of Lee, Yang, and Parr.[17]

The basis sets chosen for this study are commonly used in the electronic structure calculations of molecules. Often such basis sets are augmented with sets of polarization functions and/or diffuse functions. We have used three different polarization and diffuse functions on Pople's 6-31G basis set.[18] They are denoted as 6-31G(d,p), 6-31G(2d,2p), and 6-31 + G(d,p), where the polarization function on heavy atoms (hydrogen) is given as the first (second) argument in the parenthesis, and a set of diffuse s- and p-functions on heavy atoms is denoted as +.

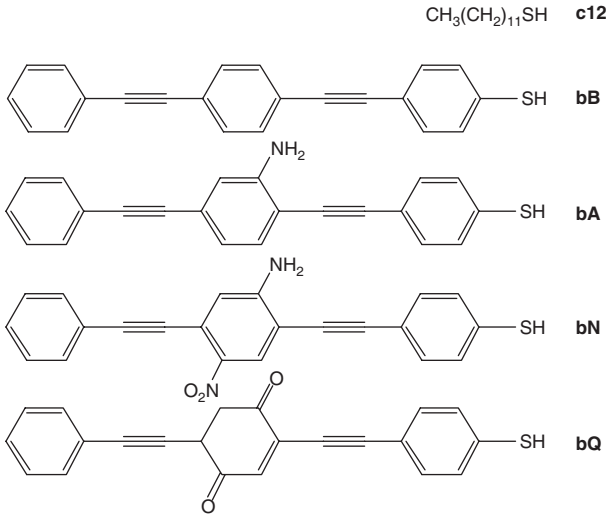

Scheme 1. Molecules examined.

Additionally, we have used correlation consistent basis sets of Dunning,[19] and they are cc-pVDZ, aug-cc-pVDZ, cc-pVTZ, and cc-pVQZ. These basis sets all include polarization functions in increasing order. Respectively, they are a set of (d functions), (polarization d and diffuse s, p, and d functions), ($2d$ and f), ($3d$, $2f$, and $1g$) functions.

The molecules examined for correlating the conduction characteristics in this study, are shown in Scheme 1. These molecules are chosen since they have been studied for their conduction characteristics by a number of groups and with various techniques.[20] The molecules, (except the 12-C chain thiol, labeled as **c12**) belong to a class of molecules called phenylene ethynylene oligomers, and are labeled as **bB**, **bA**, **bN**, and **bQ**. A different substitution in the middle phenyl ring (respectively, –H, $–NH_2$, $–NH_2$, and $–NO_2$, and =O) changes its lowest conduction channel. Geometries of these molecules are optimized at the RHF/6-31G(d) level of theory. The B3LYP/6-31G(d) canonical and VVOs are obtained at the RHF/6-31G(d) geometry.

All calculations performed in this study utilized GAMESS quantum chemistry package,[21] which includes new subroutines for computing the VVOs.

3. RESULTS AND DISCUSSION

3.1. VVOs of Nitrobenzene

The HOMO-LUMO gap is important in molecular electronics in that the location of the Fermi levels of the electrodes is near the middle of the gap in the case of zero applied potential. The LUMO energy is thought of as an indicator of the energy of the first conducting orbital that is in resonance with the energy of the electrons in the higher energy electrode when a voltage is applied, as shown in Figure 1.

Since the virtual space of the Hartree-Fock and DFT methods is not optimized, it would be interesting to see

Table I. Comparison of HOMO-LUMO gap calculated by different methods. The values in the table are in eV.

	RHF		B3LYP	
Basis set	Canonical	VVOs	Canonical	VVOs
6-31G(d,p)	11.6	12.6	5.4	5.8
6-31G(2d,2p)	11.7	12.8	5.5	5.9
6-31+G(d,p)	11.2	12.6	5.3	5.7
cc-pVDZ	11.6	12.7	5.5	5.9
aug-cc-pVDZ	10.8	12.6	5.3	5.8
cc-pVTZ	11.5	12.8	5.4	5.9
cc-pVQZ	11.5	12.8	5.4	5.9

how the HOMO-LUMO gap, obtained by the usual means (labeled as canonical in the following tables and figures) and by using the VVOs method, changes with respect to the basis set.

Table I shows a comparison of the HOMO-LUMO gap as computed from canonical orbitals and VVOs with different basis sets for HF and DFT. The canonical HOMO-LUMO gaps obtained by the HF theory vary in value with different basis sets more than those obtained by the VVOs. The HOMO-LUMO gap obtained at the DFT level shows only small variability between basis set for both the canonical and the VVOs. The VVOs method for both the HF and DFT methods always increases the HOMO-LUMO gap in comparison to the canonical orbitals.

As a higher voltage is applied to the system in Figure 1, the difference in the chemical potentials of the two electrodes becomes larger. Hence, the virtual orbitals other than LUMO of the junction molecules can become in resonance with the electrons possessing the energy higher than μ_f. Let us now look at the low-lying unoccupied orbitals. The lowest ten virtual orbitals, as well as highest ten occupied orbitals of nitrobenzene are shown in Figure 2. It was not mentioned in the preceding section, but Figure 2 shows that the QUAMBO method recovers the orbital energies of the occupied space.

It is clear from Figure 2 that the canonical virtual orbitals are basis set dependent. In particular, the orbitals calculated with a set of diffuse *s*- and *p*-functions on heavy atoms are more closely spaced in energies. This fact is evident in both the RHF and DFT calculations with the 6-31 + G(d,p) and aug-cc-pVDZ basis sets. Although not as evident as the basis with diffuse functions, the similar trend is also observed in systematically increasing the size of basis sets from cc-pVDZ to cc-pVTZ, and to cc-pVQZ. The trend is particularly evident in the RHF results. The reason for such behavior comes from the fact that the higher principal quantum number AOs in the case of the basis set with diffuse functions and the higher angular momentum AOs in the case of the larger basis set with more polarization functions have larger weights in the LCAO expansion, thereby constructing the MOs with no valence character. For example, the orbital that is one higher than the LUMO (LUMO + 1 orbital) of the VVOs

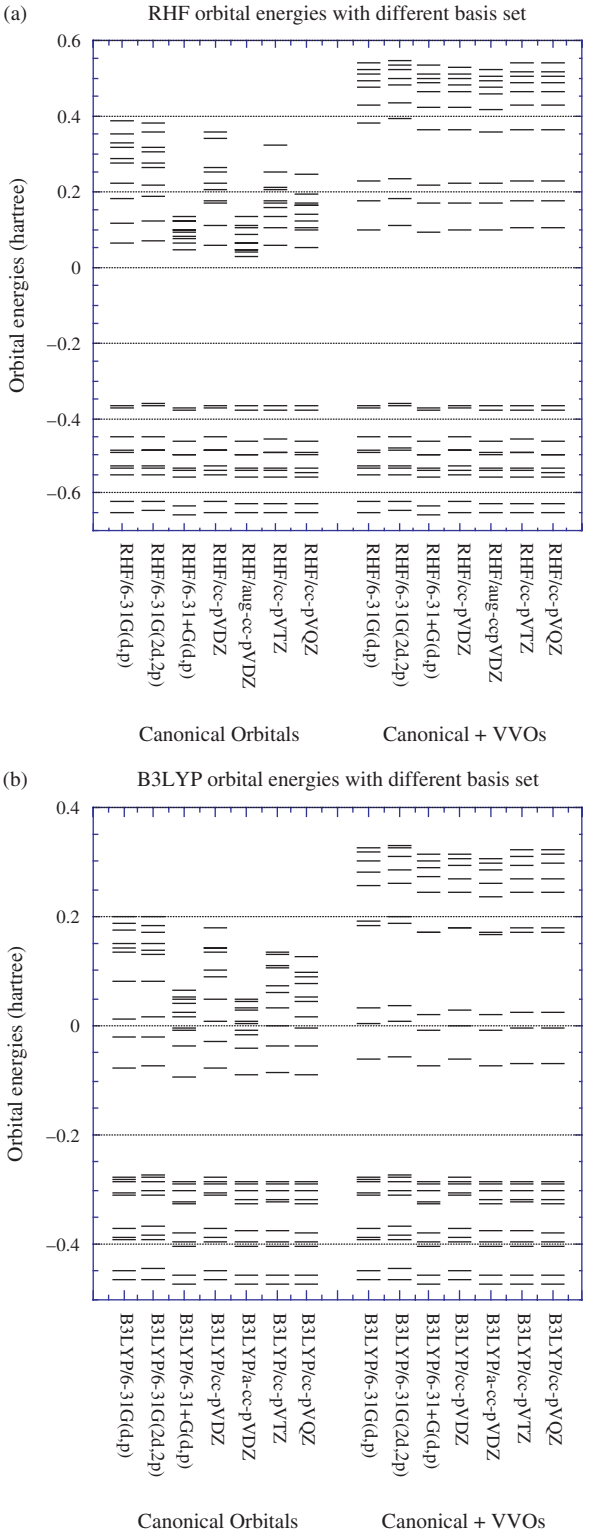

Fig. 2. Comparison of orbital energies between canonical and VVOs with different basis sets. Orbital energies of (a) RHF and (b) B3LYP are shown. Ten highest occupied orbitals and ten lowest virtual orbitals are included.

calculated at the RHF/6-31 + G(d,p) level of theory, does not appear in the canonical orbital set until the LUMO + 4 orbital of at the same level of theory. In fact, there are

RESEARCH ARTICLE

only three orbitals of valence character in the canonical set within the lowest ten MOs. The virtual canonical orbitals determined by the B3LYP/6-31+G(d,p) method have better valence characteristics in comparison with the RHF/6-31+G(d,p) level. The first three canonical orbitals have valence characteristics, as is reflected in the energetics of these orbitals. The three orbitals show qualitatively similar energy spacing as found for the corresponding VVOs. The rest of the canonical virtual orbitals have non-valence character strongly mixed in, and again this fact is reflected in the energetics; these canonical virtual orbitals are much lower in energy than those of the VVOs.

Similar intrusion of non-valence character into the canonical virtual orbitals occurs in the correlation consistent basis set. On the other hand, the VVOs of both RHF and B3LYP are remarkable stable energetically with respect to change in basis set. In nitrobenzene, there are total of nine π valence orbitals of which four are unoccupied. The lowest three VVOs possess π character, and form a low-lying orbital group. Another π orbital is energetically placed at fifth lowest, but close to the fourth σ orbital. These are close to what we expect from simple bonding theory.

3.2. Conduction Characteristics

Let us see now if we can find a trend in conduction characteristics over the various molecular species. We have chosen molecules for this study by considering the phenylene ethynylene oligomers and C-12 hydrocarbon thiol shown in Scheme 1, since these molecules have been measured for their conduction characteristics in a single article.[22] We felt that this is quite important in comparing the conduction characteristics at this juncture. Figure 3 shows the comparison between the canonical virtual orbitals and the VVOs obtained at the RHF/6-31G(d) and B3LYP/6-31G(d) levels. From the preceding section we know that the canonical orbitals of the 6-31G(d) basis set should perform quite well against the VVOs, and it is indeed the case.

c12 does not have orbitals with the π character, therefore it is seen that the virtual orbitals are higher in energy than those with the π orbital character. All other molecules possess π^* orbitals. **bB** and **bA** are without extra π orbitals. An amino group in **bA** only contributes by adding a lone pair to the system, but not π^* orbitals. The nitro group in **bN** introduces three extra (extra in comparison to **bB**) sets of π orbitals, two of which are doubly occupied, and **bN** is expected to have low-energy LUMO. In **bQ**, two extra sets of π orbitals are present with one of them doubly occupied.

Figure 3 shows the canonical and VVOs orbital energies of the highest ten occupied and the lowest ten unoccupied orbitals evaluated at the RHF/6-31G(d) and B3LYP/6-31G(d) levels of theory. As mentioned above, **c12** has wider HOMO-LUMO gap, and the occupied (unoccupied) orbitals are relatively lower (higher) than the

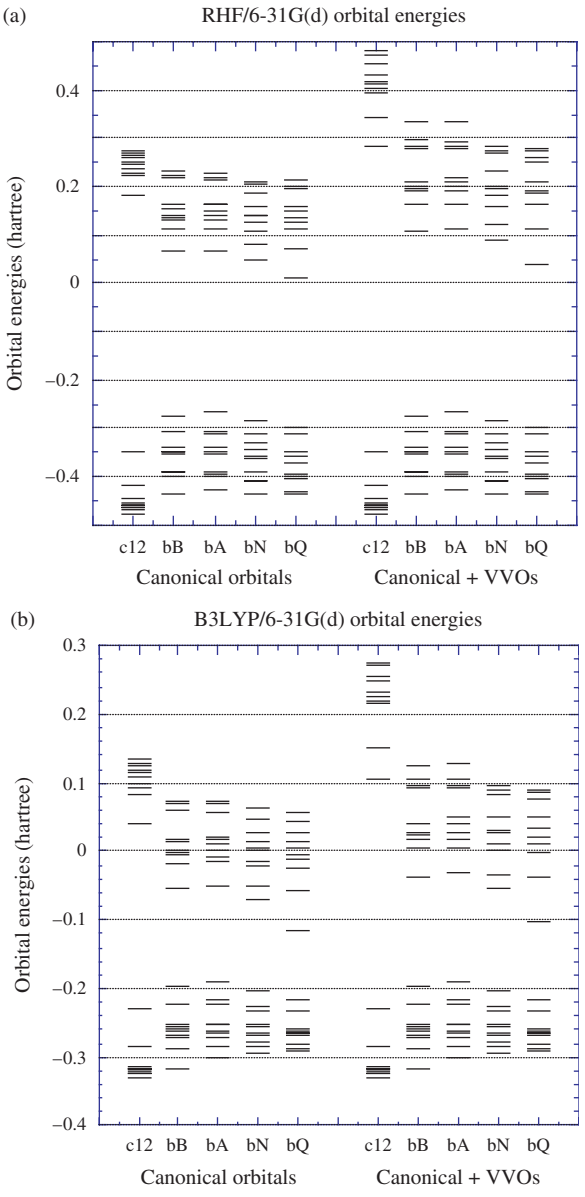

Fig. 3. Comparison of orbital energies between canonical and VVOs of various molecules. Orbital energies of (a) RHF/6-31G(d) and (b) B3LYP/6-31G(d) are shown. Ten highest occupied orbitals and ten lowest virtual orbitals are included. The molecular species labeled as **c12**, **bB**, **bA**, **bN**, and **bQ** are described in the body of text and shown in Scheme 1.

others with the π orbitals. The substituent on the central phenyl ring changes the orbital energies. The energies of HOMO of **bB**, **bA**, **bN**, and **bQ** change less than those of the LUMO at a given level of theory.

Given the description of conduction in Figure 1, we now correlate the LUMO energies with the experimental conduction measurement of Ref. [22]. The authors of that study used a tuning fork-based scanning probe microscopy (SPM) for the molecules forming self-assembled monolayer (SAM) on a gold surface. The molecules used by the SPM measurement are slightly different from ours.

RESEARCH ARTICLE

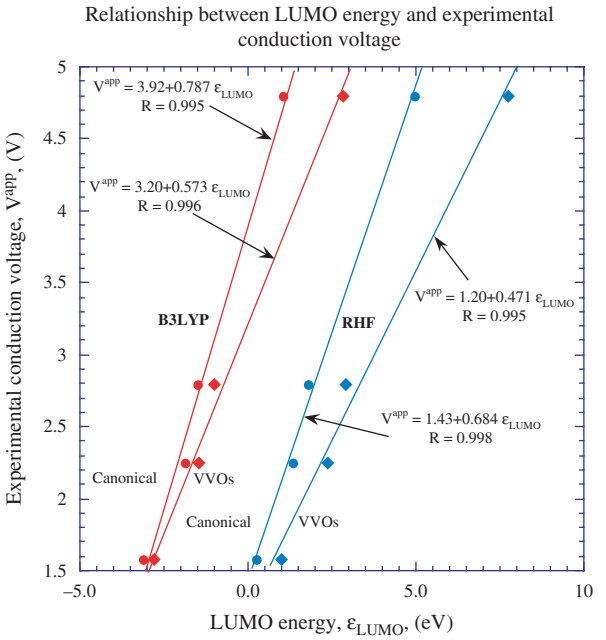

Fig. 4. Linear relationship between LUMO energy and experimental conduction voltage. The experimental points are from Ref. [22]. The two sets of data on right are obtained with the RHF/6-31G(d) method, and the left two are obtained with the B3LYP/6-31G(d) method. The circles and diamonds represent canonical orbitals and VVOs, respectively. The lines in the graphs are the results of the linear fit and their respective linear functions with the goodness of fit, *R*, are also shown.

The thiol hydrogens of the four molecules in the present studies are replaced with the acetate group. Their molecular equivalent of our **bB** possesses an ethyl group substituted for one of the hydrogens in the middle phenyl ring. Their **bN** equivalent molecule does not have amine group para to the nitro group. Despite these differences, the correlation between conduction voltage and the LUMO energy should be quite reasonable, since these differences do not change the π orbital system of the molecules significantly. Figure 4 shows a plot of the conduction voltage reported in Ref. [20] as a function of LUMO energies. In the figure, the circles (diamonds) represent the canonical orbitals (VVOs) of the four molecules, **c12**, **bB**, **bN**, and **bQ**. The right (left) two sets of data are from the RHF/6-31G(d) (B3LYP/6-31G(d)) level. The lines are the linear fit to the data. The fit to the linear relation $V^{app} = V^0 + c \cdot \varepsilon_{LUMO}$, where V^{app} is the experimental conduction voltage in volts, and ε_{LUMO} is the LUMO energy in electron volts, and c is the proportionality constant, is very good, represented by the values of R, the goodness of fit. The two canonical orbital data have a similar slope, as with the two VVOs data, indicating the LUMOs calculated by the 6-31G(d) basis are equally good in calculating the canonical and VVOs. This is consistent with the result obtained in the previous section.

The correlation shown above can be used to screen molecules for determining desired conduction voltage for designing a molecular circuit. Further, multiple conduction channels may be considered in the experiment by knowing the energetic location of low-lying LUMOs from the VVOs.

4. CONCLUSION

We have shown that the VVOs method obtains consistent virtual orbitals using different basis sets. In particular, the basis set dependence is eliminated even from the basis set with multiple polarization and the diffuse functions are present. For the VVOs as well as the canonical orbitals, the HOMO-LUMO gaps are calculated to be nearly constant among different basis sets with a given method.

The LUMOs of the molecules studied, including a hydrocarbon and four different substituted phenylene ethynylene oligomers, have a linear relation with the first conduction channel observed in the published experiments of Ref. [22].

Acknowledgments: The author wishes to acknowledge Prof. Klaus Ruedenberg for insightful and helpful discussions on QUAMBO (and others) when the author visited Ames during his sabbatical semester. The author would also like to acknowledge Dr. Michael Schmidt for his hospitality and for making the VVOs code in GAMESS available to the author. Funding from Sony Corporation and a sabbatical leave from Long Island University is gratefully acknowledged.

References

1. (a) G. Cuniberti, K. Richter, G. Fagas (eds.), Introducing Molecular Electronics, Lecture Notes in Physics, Springer, Berlin/Heidelberg **(2005)**, Chaps. 2 and 5, Vol. 680; (b) S. Datta, Quantum Transport, Atom to Transistor, Cambridge University Press, Cambridge **(2005)**; (c) R. Lake and S. Datta, *Phys. Rev. B* 45, 6670 **(1992)**.
2. V. Mujica, M. Kemp, and M. A. Ratner, *J. Chem. Phys.* 101, 6849 **(1994)**.
3. T. Shimazaki, Y. Xue, M. A. Ratner, and K. Yamashita, *J. Chem. Phys.* 124, 114708 **(2006)**.
4. M. Brandbyge, J.-L. Mozos, P. Ordejón, J. Taylor, and K. Stokbro, *Phys. Rev. B* 65, 165401 **(2002)**.
5. Y. Xue and M. A. Ratner, *Phys. Rev. B* 68, 115406 **(2003)**.
6. S.-H. Ke, H. U. Baranger, and W. Yang, *Phys. Rev. B* 70, 085410 **(2004)**.
7. C. Gonzales and R. G. E. Morales, *Chem. Phys.* 250, 279 **(1999)**.
8. (a) N. Matsunaga and K. Sohlberg, *J. Nanosci. Nanotechnol.* 2, 659 **(2002)**; (b) N. Matsunaga and K. Sohlberg, *J. Nanosci. Nanotechnol.* 1, 275 **(2001)**.
9. N. Carroll and K. Sohlberg, *Mater. Res. Soc. Symp. Proc.* 734, B9.63 **(2002)**; (b) N. Vedova-Brook, N. Matsunaga, and K. Sohlberg, *Chem. Phys.* 299, 89 **(2004)**.
10. D. M. Adams, L. Brus, C. E. D. Chidsey, S. Creager, C. Creutz, C. R. Kagan, P. V. Kamat, M. Lieberman, S. Lindsay, R. A. Marcus, R. M. Metzger, M. E. Michel-Beyerle, J. R. Miller, M. D. Newton, D. R. Rolison, O. Sankey, K. S. Schanze, J. Yardley, and X. Zhu, *J. Phys. Chem. B* 107, 6668 **(2003)**.

RESEARCH ARTICLE

11. (a) R. B. Woodward and R. Hoffmann, The Conservation of Orbital Symmetry, Verlag Chemie and Academic Press, Weinheim and New York **(1970)**; (b) R. Hoffmann, *Acc. Chem. Res.* 4, 1 **(1971)**; (c) R. Hoffmann and R. B. Woodward, *Acc. Chem. Res.* 1, 17 **(1968)**.
12. (a) K. Fukui, T. Yonezawa, and H. Shingu, *J. Chem. Phys.* 20, 722 **(1952)**; (b) K. Fukui, T. Yonezawa, C. Nagata, and H. Shingu, *J. Chem. Phys.* 22, 1433 **(1954)**; (c) K. Fukui, T. Yonezawa, and C. Nagata, *Bull. Chem. Soc. Jpn.* 27, 423 **(1954)**; (d) K. Fukui, T. Yonezawa, and C. Nagata, *J. Chem. Phys.* 26, 831 **(1957)**; (e) K. Fukui, T. Yonezawa, and C. Nagata, *J. Chem. Phys.* 27, 1247 **(1957)**; (f) *Acc. Chem. Res.* 4, 57 **(1971)**.
13. (a) F. Bernardi, M. Olivucci, and M. A. Robb, *Acc. Chem. Res.* 23, 405 **(1990)**; (b) K. N. Houk, J. Gonzalez, and Y. Li, *Acc. Chem. Res.* 28, 81 **(1995)**.
14. (a) W. C. Lu, C. Z. Wang, M. W. Schmidt, L. Bytautas, K. M. Ho, and K. Ruedenberg, *J. Chem. Phys.* 120, 2629 **(2004)**; (b) *ibid.* 2638.
15. P. J. Stephens, F. J. Devlin, C. F. Chabalowski, and M. J. Frisch, *J. Phys. Chem.* 98, 11623 **(1994)**.
16. A. D. Becke, *J. Chem. Phys.* 98, 5648 **(1993)**.
17. C. Lee, W. Yang, and R. G. Parr, *Phys. Rev. B* 37, 785 **(1988)**.
18. For H and 2nd row elements; W. J. Hehre, R. Ditchfield, and J. A. Pople, *J. Chem. Phys.* 56, 2257 **(1972)**, for 3rd row elements, M. M. Francl, W. J. Petro, W. J. Hehre, J. S. Binkley, M. S. Gordon, D. J. DeFrees, and J. A. Pople, *J. Chem. Phys.* 77, 3654 **(1982)**.
19. For H and 2nd row elements; T. H. Dunning, Jr., *J. Chem. Phys.* 90, 1007 **(1989)**, for 3rd row main group elements; D. E. Woon and T. H. Dunning, Jr., *J. Chem. Phys.* 98, 1358 **(1993)**.
20. (a) M. A. Reed, C. Zhou, C. J. Muller, T. P. Burgin, and J. M. Tour, *Science* 278, 252 **(1997)**; (b) J. Chen, M. A. Reed, A. M. Rawlett, and J. M. Tour, *Science* 286, 1550 **(1999)**; (c) J. Chen, W. Wang, M. A. Reed, A. M. Rawlett, D. W. Price, and J. M. Tour, *Appl. Phys. Lett.* 77, 1224 **(2000)**; (d) Z. J. Donhauser, B. A. Mantooth, T. P. Pearl, K. F. Kelly, S. U. Nanayakkara, and P. S. Weiss, *Jpn. J. Appl. Phys.* 41, 4871 **(2002)**.
21. M. W. Schmidt, K. K. Baldridge, J. A. Boatz, S. T. Elbert, M. S. Gordon, J. H. Jensen, S. Koseki, N. Matsunaga, K. A. Nugyen, S. Su, T. L. Windus, M. Dupuis, and J. A. Montgomery, *J. Comput. Chem.* 14, 1347 **(1993)**.
22. F.-R. F. Fan, J. Yang, S. M. Dirk, D. W. Price, D. Kosynkin, J. M. Tour, and A. J. Bard, *J. Am. Chem. Soc.* 123, 2454 **(2001)**.

Received: 10 July 2006. Accepted: 14 July 2006.